



Biophotonic tools for probing extracellular matrix mechanics



B. E. Sherlock ^{a *}, J. Chen ^b, J. C. Mansfield ^b, E. Green ^b and C. P. Winlove ^b

a - College of Medicine and Health, University of Exeter, Exeter EX1 2LU, United Kingdom

b - College of Engineering, Mathematical and Physical Sciences, University of Exeter, Exeter EX4 4QF, United Kingdom

Correspondence to B.E. Sherlock: b.sherlock@exeter.ac.uk (B.E. Sherlock)

<https://doi.org/10.1016/j.mplus.2021.100093>

Abstract

The complex, hierarchical and heterogeneous biomechanics of the extracellular matrix (ECM) are central to the health of multicellular organisms. Characterising the distribution, dynamics and above all else origins of ECM biomechanics are challenges that have captivated researchers for decades. Recently, a suite of biophotonics techniques have emerged as powerful new tools to investigate ECM biomechanics. In this mini-review, we discuss how the non-destructive, sub-micron resolution imaging capabilities of Raman spectroscopy and nonlinear microscopy are being used to interrogate the biomechanics of thick, living tissues. These high speed, label-free techniques are implemented during mechanical testing, providing unprecedented insight into the compositional and structural response of the ECM to changes in the mechanical environment.

© 2021 The Author(s). Published by Elsevier B.V. This is an open access article under the CC BY-NC-ND license (<http://creativecommons.org/licenses/by-nc-nd/4.0/>).

Introduction

The extracellular matrix (ECM) is a complex, 3D network of fibrous proteins immersed in a proteoglycan rich fluid that fills the spaces between cells. The biomechanical properties of the ECM play a critical role in the development and maintenance of organ tissues. In addition to providing a structural scaffold to support cell adhesion and migration, the ECM provides chemical and mechanical cues that influence cell behaviour [1]. Much of our current understanding of ECM biomechanics derives from mechanical testing of macroscopic samples followed by wet biochemical analysis and light or electron microscopy to provide structural information. Whilst significant progress continues to be made using these tools, there are at least two important areas related to the complexity of the ECM that challenges their ability to provide new insight. First, it is clear that tissues are so heterogeneous that structure-function relationships must be investigated on a microscopic

scale, and second, understanding the dynamic mechanical interactions between cells and matrix is central to understanding tissue physiology and pathology. The aim of this mini-review is to highlight how rapidly evolving optical imaging and spectroscopic techniques are being used to make measurements of ECM biomechanics that address the challenges of both areas.

We have chosen to focus this mini-review on two complementary methodologies, Raman spectroscopy and nonlinear microscopy, that characterise the chemical composition and structure of the ECM. Both techniques are compatible with deployment during mechanical testing of fresh tissue samples, allowing real-time monitoring of the load-induced microscopic tissue response. In concentrating on the ECM, we shall not specifically address cellular biomechanics, nor the burgeoning field of mechanotransduction on which topics several high-quality reviews have recently been published [2–5]. Space also precludes consideration of other highly promising

optical techniques such as optical coherence elastography [6], and Brillouin microscopy [7]. Finally, we also neglect the significant contribution of \times ray diffraction which, using synchrotron sources is beginning to provide information on tissue mechanics at the molecular level [8].

Following a brief technical overview of Raman spectroscopy and nonlinear optical microscopy, we shall focus firstly on the application of these techniques to study the influence of ECM biochemistry on its mechanical properties, and secondly on the relationship between macroscale biomechanics and ECM microstructure.

Technical background

Raman spectroscopy

Molecules possess a discrete spectrum of vibrational modes that are determined by the type, strength and distribution of bonds within the molecule. A measurement of this vibrational spectrum can be used to identify the molecule and furthermore, to infer its abundance, organisation or local mechanical environment [9]. When light is scattered by a biological sample, a small but measurable number of photons are frequency shifted by their interaction with the vibrational modes of the sample [10]. By recording this frequency shift, Raman spectroscopy provides an indirect measurement of the spectrum of molecular vibrational modes in a local region of the sample [11]. The compositional data reported by Raman spectroscopy has been used to study a variety of key tissue components including glycosaminoglycans (GAGs) [12], lipids [13], hydroxyapatite [14], DNA [15], elastin [16] and the conformational state of collagen [17]. Raman spectrometers can be readily integrated with confocal or laser scanning microscopes [18]. In this configuration, Raman spectra can be acquired from a region of the sample, allowing the construction of a depth-resolved hyperspectral image that illustrates the spatial distribution of the sample composition. The left hand panel of Fig. 1 is a diagram of a generic Raman spectroscopy setup. Although many variants of this configuration have been developed over the years, the setup in Fig. 1. depicts the core elements of a Raman spectrometer, namely: A continuous wave laser that illuminates the sample; optical elements such as filters and dichroic beamsplitters to separate the Raman scattered photons from scattered and reflected light at the incident frequency; and a spectrometer to disperse the Raman signal into its spectral components and detect them separately (done using a diffraction grating and linear CCD detector in the figure).

A significant drawback of Raman spectroscopy is the speed of data acquisition. Raman scattering is a weak process that requires long acquisition times to capture spectra with sufficient signal to noise to be useful [19,20]. Coherent Raman Scattering (CRS)

microscopy is a suite of rapidly evolving techniques that probe the Raman spectra of samples, but afford several orders of magnitude improvement in data acquisition rates over conventional Raman spectroscopy [21,22]. Although there are trade-offs to be made between the acquisition time and resolution of the acquired spectra, as long ago as 2005, CRS has been able to perform video rate biochemical imaging [23]. All CRS techniques employ two laser beams, emitting ultrashort ($<1 \times 10^{-11}$ s) pulses of light that are focussed onto the same region of the sample. The optical frequency difference between the lasers is tuned to equal a single Raman active mode of a molecular species of interest. This leads to the coherent excitation of this Raman mode and the generation of an optical signal with sufficient strength to be used for imaging. Two CRS techniques commonly used for biological imaging are coherent anti-Stokes Raman scattering (CARS) [24] and stimulated Raman scattering (SRS) [25]. Early realisations of these techniques were limited to probing a single Raman band per image. However, recent developments in rapid wavelength scanning have enabled the high-speed acquisition of hyperspectral images that combine sub-micron resolution, with a broad spectral range e.g. 200–1500 cm^{-1} [26,27].

Nonlinear microscopy

Nonlinear microscopy is the name given to the collection of techniques that excite and detect light generated via the nonlinear optical response of the sample [28]. The etymology here derives from the nonlinear relationship between the intensities of the illumination and detected signal. In conventional light microscopy, this relationship is approximately linear (i.e. doubling the illumination intensity doubles the brightness of the image). However, in e.g. second harmonic generation (SHG), one of the most widely used form of nonlinear microscopy, the intensity of the detection varies with the square of the illumination intensity [29]. Nonlinear optical processes require the near simultaneous arrival of two or more photons to the same location within the sample in order to be excited [30]. Thus, in nonlinear microscopy, samples are illuminated with ultrafast pulsed laser systems, where the tight packing of incident light into time intervals that typically range between 10 picoseconds down to 10 fs, significantly increases the chances of simultaneous photon arrival events. To further increase the efficiency of nonlinear microscopy, all the incident light is focussed down into a volume, the dimensions of which are typically only a few hundred nanometres in any direction. This high spatial concentration of laser light results in the vast majority of the nonlinear microscopy signal originating from this focal volume [31]. As a result, nonlinear microscopy possesses an intrinsic depth-sectioning capability, that is similar to a confocal microscope, but doesn't require a pinhole in the emission pathway. More-

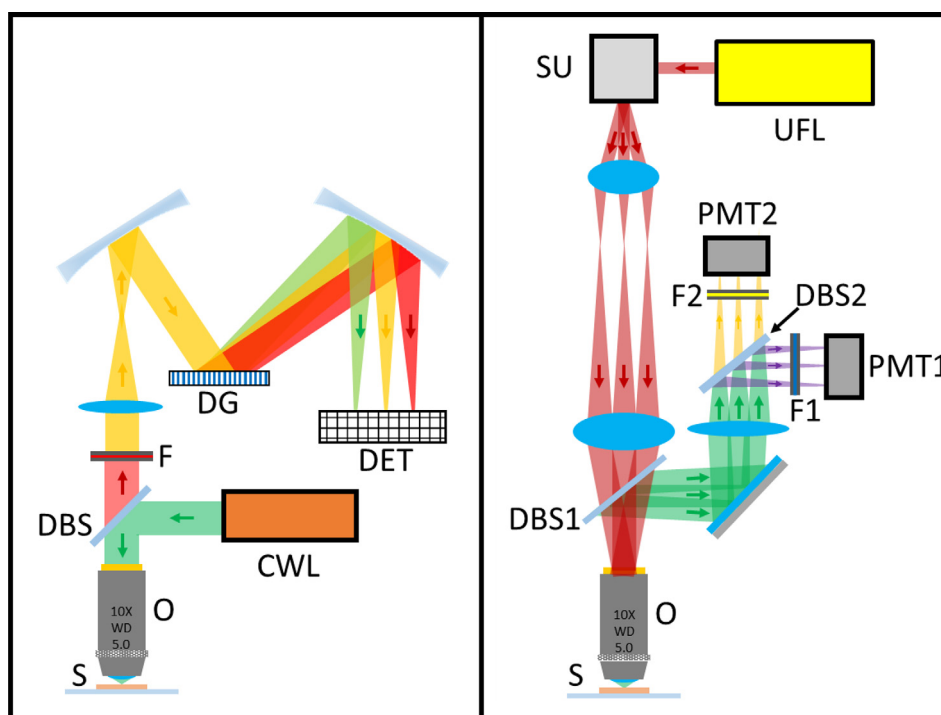


Fig. 1. (Left) Schematic diagram of a Raman spectrometer. CWL: Continuous wave laser; DBS: Dichroic beamsplitter; DET: CCD detector; DG: Diffraction grating; F: Filter; O: Objective; S: Sample. (Right) Schematic diagram of a nonlinear microscope. DBS1 & DBS2: Dichroic beamsplitters; F1 & F2: Filters; O: Objective; PMT1 & PMT2: Photomultiplier tubes; S: Sample; SU: Scanning unit; UFL: Ultrafast laser.

over, the use of near-infrared light for illumination allows nonlinear microscopy to image deeper below the sample surface, and potentially cause less photodamage to the sample than the visible light used in conventional fluorescence microscopy [32,33].

Nonlinear microscopy is widely used to image the distribution of exogenous probes in biological samples [34,35]. However, it is equally adept at acquiring images using only endogenous contrast, and it is this latter category that we focus on during this mini-review. On a molecular scale, the non-centrosymmetric and highly crystalline nature of fibrillar collagen make them a strong emitter of SHG light [36]. Indeed SHG microscopy has now become the gold standard for imaging the microstructure of unstained collagen [37]. In addition to collagen, microtubules [38], myosin [39] and amylopectin [40] are all routinely imaged using SHG. Two-photon excited fluorescence (TPEF) is closely related to, and often acquired in parallel with SHG [41]. In TPEF, the near simultaneous absorption of two coincident photons induces a transition to higher molecular energy state. The subsequent decay to the molecular ground state is mediated by the emission of a photon. In the ECM, elastin fibres [42] and collagen crosslinks [43] are the primary sources of endogenous TPEF contrast. The CRS techniques discussed in the previous section are also types of nonlinear microscopy. The right hand panel of Fig. 1 is a schematic diagram of a

laser scanning nonlinear microscope setup. The instrument depicted is configured for excitation and detection of TPEF and SHG. Additional components and a more complex beam path are required for acquiring CRS images. However, the setup in Fig. 1 shows many of the elements that are common to all nonlinear microscopes, such as: An ultrafast laser used for illumination; a scanning unit, the action of which cause the focal spot of the objective lens to be scanned across the sample plane, a dichroic beamsplitter to separate incident from emitted light, and one or more highly sensitive detectors often responsible for detecting different spectral regions of the sample emission. Examples of nonlinear microscopy images, acquired using SHG, TPEF and SRS from fresh, unlabelled tissue sections are shown in Fig. 2.

Polarisation sensitivity

The signal generated in both Raman spectroscopy and nonlinear microscopy is sensitive to the relative alignment of the polarisation axis of the incident light, and the overall orientation of the molecular ensemble being imaged [44]. For example, in polarisation sensitive SHG microscopy, the intensity of the SHG signal can drop to almost zero when the light polarisation is rotated perpendicular to the direction of a well organised, uniaxial distribution of collagen

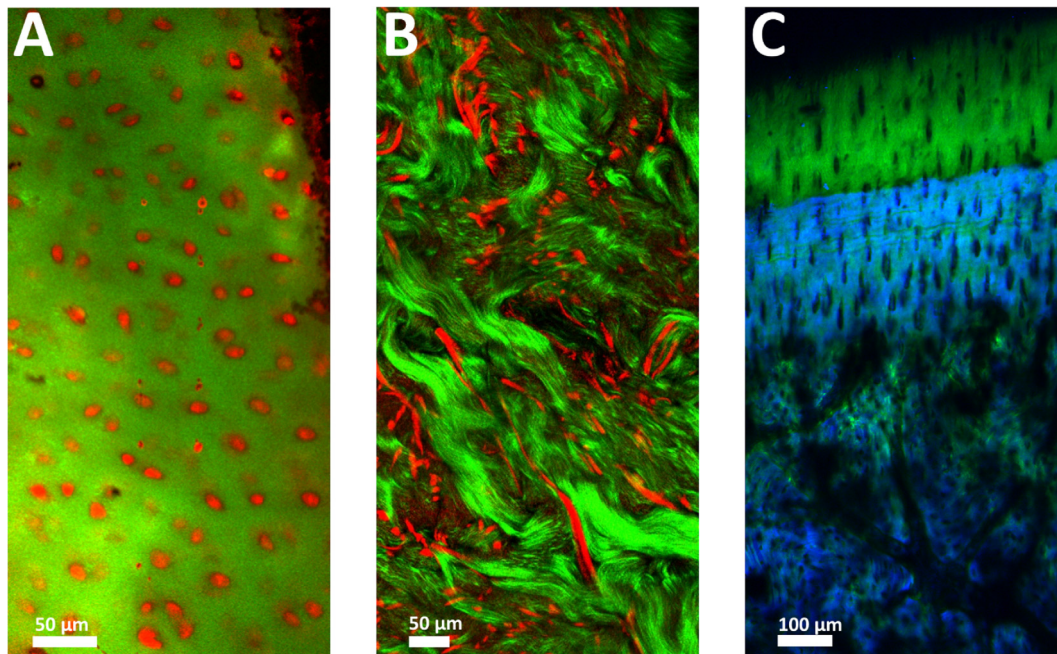


Fig. 2. Nonlinear microscopy images acquired from fresh, thick, unstained tissue samples. A) Bovine articular cartilage imaged using the second harmonic generation (SHG) from fibrillar type II collagen (green) and cellular two-photon excited fluorescence (TPEF) (red) B) Image of the dermal layer of human skin, consisting of collagen SHG (green) and elastin TPEF (red). C) Boundary between calcified cartilage and subchondral bone in the equine metacarpophalangeal joint. Here the image depicts the collagen SHG (green) and the stimulated Raman scattering phosphate peak (blue), indicating the presence of mineral. (For interpretation of the references to colour in this figure legend, the reader is referred to the web version of this article.)

fibrils [45]. Far from being a hindrance, this polarisation dependence can probe the organisation of tissue on lengths scales far smaller than the optical resolution limit. This can be understood by considering the organisation of collagen fibrils at each pixel in the SHG image. Where the tissue is well organised, with the majority of collagen fibrils aligned along the same direction, the intensity of the SHG signal will be strongly modulated by rotating the optical polarisation axis. However, for the pixels that correspond to regions of low organisation, where no dominant fibril orientation exists, rotating the polarisation axis of the incident light will have little or no impact on the SHG intensity. The reason for this is that no matter the orientation of polarisation, there will always be approximately the same number of fibrils that are aligned with this direction that will emit an SHG signal. Thus, even though the nanometre scale organisation of collagenous tissues is below the optical resolution limit and so not directly visible in the SHG image, polarisation sensitive SHG can be used to record a measure of tissue structure at this length scale. Thus, polarisation sensitive techniques simultaneously image structure and composition at the microscopic scale, and report a measure of organisation at the molecular scale.

The approaches covered in this mini-review fall into two categories: Correlative and mechanistic. In the correlative studies e.g. [46–50], parameters

extracted from optical images are calibrated against conventional measurements of sample biomechanics. Once this analysis is complete, optical techniques can serve as a fast, non-destructive proxies for the conventional measurements of tissue biomechanics. Correlative studies are often motivated by the need for longitudinal monitoring of changes in tissue composition, structure, and function. This is particularly important in fields such as tissue engineering, where the maturation protocol can be adapted to optimise mechanical properties, and samples can be measured against biomechanical “release criteria” prior to implantation. Mechanistic studies use parameters extracted from optical images to explain the origins of macroscopic tissue biomechanics e.g. [51–55]. In these experiments, optical measurements of structural and/or compositional adaptations of tissue in response to changes to the local mechanical environment are combined within a theoretical framework to develop structural models of tissue mechanics.

The relationship between ECM biomechanics and biochemistry

Much of our current understanding of ECM biomechanics derives from research into its chemical composition. Biochemical assays such

as high performance liquid chromatography or enzyme-linked immunosorbent assays are tried and trusted tools for studying the biochemical makeup of the ECM. By running these assays on samples that have previously undergone mechanical testing, relationships between composition and biomechanics are probed. However, biochemical assays are destructive, prohibiting longitudinal studies of the same sample, and do not provide information on the spatial distribution of matrix components. By contrast, the biophotonic tools discussed in this mini-review offer both of these capabilities. In this section, examples of their application to specific problems in matrix biology are discussed.

Tissue engineering applications

Raman spectroscopy has been used to study zonal differences in the composition and biomechanics of native and engineered articular cartilage [56]. In this correlative study, the authors used multivariate statistical analysis to map the relative abundances of 5 different components of cartilage across the different cartilage zones. By correlating their results with a nanoindentation dataset the authors concluded that cartilage microstructure, rather than composition had the dominant impact on zonal biomechanics. A related study showed that similar measurements of cartilage composition can be acquired using SRS, with the accompanying order of magnitude decrease in image acquisition time [57]. Zhuo *et al* used a combination of SHG and CARS microscopy to perform a correlative study into the crosslinking process in engineered bone constructs [46]. The authors observed the SHG images of bone constructs encoded information on the degree of crosslinking, which correlated with bulk elastic modulus. Furthermore, a combination of SHG intensity and CARS spectral measurements were shown to correlate with crosslinking induced changes to the conformational state of the collagen triple helix. A later study by Marturano *et al* showed that lysyl oxidase induced crosslinking in embryonic chick tendon was a strong indicator of tendon biomechanics, and that TPEF could be used to monitor the crosslink density in thick, living tissue [43]. Finally in this subsection, Shaik *et al* adopted a multimodal approach to imaging degradative changes in the composition and mechanics of equine pericardium during digestion by bacterial collagenase [58]. A combination of Raman spectroscopy and nonlinear microscopy allowed the authors to make longitudinal measurements of the decrease in collagen content, and the corresponding changes in pericardium mechanics during digestion.

Tissue specific applications

The role played by GAGs in determining the mechanics of arterial ECM was investigated by

Mattson *et al* [59]. By analysing SHG and TPEF images acquired from arterial tissue undergoing biaxial tensile testing, the authors found that GAG removal has an important impact on the passive mechanical properties of the tissue. Specifically, they showed that following GAG removal, collagen fibres were straighter, and both collagen and elastin fibres were recruited earlier during mechanical loading. In a recent study by Labroo *et al*, compositional parameters derived from Raman spectroscopy were used explain differences in the biomechanics of fresh human and swine skin samples [60]. Here the authors used the Raman spectra to measure the ratio of collagen to elastin in their samples. These compositional measurements helped explain the variation in elastic modulus between skin samples that the authors measured by tensile testing. Raman spectroscopy has also been used to investigate the mechanical response of hard tissues such as bone and enamel to an applied load. Pezzotti *et al* used a Raman micro-spectrometer to study the distribution of stress when teeth were subjected to macroscopic compressive stress [61]. Shifts in the position of the hydroxyapatite peak were used to map the microscopic distribution of stress at the interface between tooth enamel and dentin. The authors observed that whilst enamel was mostly under tension, dentin was largely found in compression.

Applications in aging and disease

Nonlinear microscopy was used to study the effect of aging on arterial ECM composition and mechanics by Cavinato *et al* [55]. In this comprehensive study, the results of biaxial mechanical testing showed strong correlations with data extracted from SHG and TPEF images of murine aorta at five different ages. For example, the authors report that collagen fibre straightness and bundle width significantly correlated with circumferential and axial stiffness, and cell densities correlated negatively with passive mechanical metrics in the circumferential direction. A similar study on the compositional and functional impacts of aging on the skin was published by Pittet *et al* in 2014 [47]. The authors used nonlinear microscopy to track changes in the concentration of collagen and elastin in the human dermis as a function of age. In this correlative study, although they also reported significant heterogeneity within and between samples, the authors measured an overall decrease in relative abundance of both collagen and elastin in skin samples from old volunteers. These changes corresponded to measured changes in skin elasticity and elastic recovery.

The modification of tissue biomechanics is one of the hallmarks of cancer. In a 2018 study conducted by Brauchle *et al*, compositional data extracted by Raman spectroscopy was used to provide a key insight into the mechanism underpinning the increased stiffness of tumour over healthy human

colon tissue [62]. Specifically, the authors measured significantly elevated levels of GAGs in the collagen rich regions of tumour tissue. Although the authors show that it is collagen structure rather than GAG concentration that dictates tumour tissue biomechanics, they postulate that the presence of elevated levels of GAGs may have significantly influenced tumour collagen remodelling.

The relationship between gross sample biomechanics and microstructure.

The combination of quantitative biomechanical assays such as tension, compression or shear stress with histological imaging has provided considerable insight into the microstructural origins of tissue mechanics. However, this approach is vulnerable to sampling and processing artefacts, and only offers isolated snapshots of tissue microstructure. Nonlinear microscopy and Raman spectroscopy offer similar, or in some cases superior structural information to histological imaging, but in real-time from thick, living tissues. Furthermore, the non-destructive nature of these techniques allows them to record the dynamics of structural reorganisation in response to a change in the local mechanical environment. In this section, we will discuss some of the pioneering work that has used these optical techniques to study the relationship between tissue biomechanics and microstructure.

Tissue engineering applications

Collagen hydrogels are widely used in the field of tissue engineering. They provide a 3D biomimetic environment, in which the biochemical and biomechanical composition can be tuned to meet the requirements of specific applications. In a series of correlative studies, Raub *et al* used nonlinear microscopy to non-destructively probe the mechanical properties of acellular [63] and cellular [49] collagen hydrogels. In acellular gels, the authors found that the impact on hydrogel storage modulus of glutaraldehyde mediated crosslinking correlates with mean TPEF image intensity. Building on this work, they reported that TPEF and SHG image parameters such as skewness and speckle contrast act as good predictors for the Young's modulus of cellularised collagen hydrogels. Finally in this sub-section, a multiscale image correlation technique applied to SHG images was used to report the presence of cell mediated residual stress in unloaded collagen hydrogels [64].

Tissue specific studies

The relatively simple, collagen type (I) dominated structure, and importance to physiological function

has made tendon one of the most popular models for studying the hierarchical relationship between tissue mechanics and microstructure. Polarisation sensitive SHG was used to monitor the multiscale response of collagen fibrils from a rat tail tendon, placed under tension [54]. The authors concluded that under physiological loads, an increase in the alignment of fibrils within the tendon fascicle was the dominant contribution to sample stretching. Interestingly, the authors also reported a decrease in fibril alignment under super-physiological loading conditions, suggesting some fibrils began to break and so lose their alignment with the fascicle axis. Later, Quigley *et al* used SHG to study the structural origins of tendon biomechanics at a single fibril level [65]. The authors observed significant decrease in SHG intensity following mechanical rupture of isolated fibrils extracted from positional tendons. In contrast, fibrils extracted from energy storing tendons did not display this behaviour, indicating a greater resistance to molecular disorder that the authors attribute to greater trivalent crosslinking in energy storing tendons. SHG has also proved an indispensable tool for uncovering the microstructural origins of changes to the biomechanical properties of tendons under disease [66,67] and repair [68,69].

In addition to its role in protection and thermoregulation of the body, skin must adapt to a broad range of mechanical requirements. Raman spectroscopy has been used to study the multiscale response of the structural proteins of the skin when exposed to uniaxial strain [70]. At low strains, the authors observed that load transfer is primarily mediated by elastin and the non-helical domains of collagen. As the strain increases, the triple helix domain of collagen is increasingly recruited to assist in this process. Lynch *et al* used nonlinear microscopy to investigate the microstructural origins of mouse skin biomechanics [51]. The authors show that unlike tendon, the stretch in skin cannot be attributed to the extension of already aligned collagen fibres. Instead, the authors observed that the fraction of fibres that are aligned in the direction of traction increases throughout the tensile testing process. Woessner *et al* used a similar approach to study collagen fibre kinematics during tensile testing [71]. The authors observed a non-affine relationship between tissue deformation and collagen fibre reorientation, suggesting that fibre-fibre interactions play a significant role in skin biomechanics.

Another study used nonlinear microscopy to quantify the sequential engagement of ECM structural proteins in response to mechanical loading [52]. Specifically, TPEF and SHG were used to simultaneously monitor real-time changes in the elastin and collagen networks of arterial ECM during biaxial loading. The authors conclude that unlike the collagen network which rapidly realigns in response to mechanical loading, the elastin network remains largely unchanged. These results

suggest that arterial elastic fibres are under tension, and impart a compressive stress on the collagen network. The ability to study the dynamic interaction between matrix proteins has important consequences for the field of mechanobiology and numerical modelling of the ECM. Building on these findings, other groups have adopted the same combination of nonlinear microscopy techniques to study the formation of local strain fields in arterial elastin networks [72] and to delineate layer dependent differences in aortic collagen network responses to increased luminal pressure [73–75].

Our own research group have pioneered the use of nonlinear microscopy as a tool to probe the response of type II collagen fibrils in articular cartilage when placed under strain [76]. Initially, we used the TPEF signal from live chondrocytes to map the formation of strain fields in thick cartilage samples placed under tension. This work detected cellular scale anisotropies in the collagen network that gave rise to significant variations in the distribution of strain. We followed this paper with a study that combined images of collagen SHG with elastin TPEF to investigate the role played by elastic fibres in articular cartilage placed under external load [53]. Similar to the finding of the arterial studies discussed above, this study concluded that elastin in articular cartilage exists under tension, and that these fibres are primarily recruited when cartilage is exposed to shear or tensile loads. Finally, in a recent study we used polarisation sensitive to perform a multiscale analysis of the reorientation and reorganisation of type II collagen under tensile strain. The study found that the initial strain was largely taken up by fibre reorientation in the direction of applied strain. However, at higher strains organisational changes on a molecular scale were also observed [77].

Conclusion

Raman spectroscopy and nonlinear microscopy can be used to measure sub-micron resolution maps of the adaptations in ECM structure and composition occurring during changes in the local mechanical environment. An exciting aspect of these and other biophotonic techniques is that they are rapidly evolving. Researchers around the world are working on methods to allow images to be acquired faster [78], from deeper below the sample surface [79], and at higher resolution [80]. In combination with the more established tools of matrix biology, these techniques have the potential to drive breakthroughs in high impact challenges in biology and medicine. For example, new insights into the casual relationship between chondrocyte metabolism and compromised matrix mechanics will be key to a better understanding of the pathogenesis of osteoarthritis. Furthermore, progress in the development of functional biomaterials depends on our ability to understand and reproduce the hier-

archical origins of tissue biomechanics. Finally, accurate characterisation of the cellular scale heterogeneity in the ECM's response to a mechanical load is vitally important for advancing our understanding of the mechanisms underpinning mechanotransduction.

To fully characterise the complex, hierarchical biomechanics of the ECM, the symbiosis between experiment and computational simulation must be exploited. Currently, there are some examples in the literature of key parameters for constitutive *in silico* models of the ECM being calibrated using data acquired by optical imaging and spectroscopy [81–83]. In the future however, as the adoption of optical techniques becomes more widespread, we anticipate this approach will undergo significant growth, and so support a more comprehensive understanding of ECM biomechanics.

Finally, the ability to non-destructively image thick, living tissue without exogenous contrast means the optical techniques discussed in this mini-review can be readily deployed *in vivo*. The development of clinically compatible, handheld and endoscopic biophotonic instruments is a vibrant and rapidly advancing field [84–86]. Today, the quality of the data acquired by these instruments all but matches those acquired by traditional lab-based systems, raising the prospects for a new era of investigation into *in vivo* biomechanics. The opportunity to study the ECM response to physiological loads *in vivo* will only further advance our understanding of matrix biomechanics, and could also lead to breakthroughs in diagnosis and treatment of matrix pathologies.

DECLARATION OF COMPETING INTEREST

The authors declare that they have no known competing financial interests or personal relationships that could have appeared to influence the work reported in this paper.

Acknowledgement

This work was supported in part by funding from a Rosetrees trust seedcorn award [Ref: JS16 / M896].

Received 30 July 2021;

Accepted 11 November 2021;

Available online 18 November 2021

Keywords:

Raman spectroscopy;

Nonlinear microscopy;

Biomechanics;

Second harmonic generation;

Collagen;
Extracellular matrix mechanics, tissue engineering;
Longitudinal monitoring;
Biophotonics

References

- [1] Vining, K.H., Mooney, D.J., (2017). Mechanical forces direct stem cell behaviour in development and regeneration. *Nat. Rev. Mol. Cell Biol.*, **18** (12), 728–742. <https://doi.org/10.1038/nrm.2017.108>.
- [2] D. Mohammed *et al.*, “Innovative tools for mechanobiology: Unraveling outside-in and inside-out mechanotransduction,” *Front. Bioeng. Biotechnol.*, vol. 7, no. JUL, 2019, doi: 10.3389/fbioe.2019.00162.
- [3] Arbore, C., Perego, L., Sergides, M., Capitano, M., (2019). Probing force in living cells with optical tweezers: from single-molecule mechanics to cell mechanotransduction. *Biophys. Rev.*, **11** (5), 765–782. <https://doi.org/10.1007/s12551-019-00599-y>.
- [4] Li, M., Dang, D., Liu, L., Xi, N., Wang, Y., (2017). Atomic force microscopy in characterizing cell mechanics for biomedical applications: A review. *IEEE Trans. Nanobioscience*, **16** (6), 523–540. <https://doi.org/10.1109/TNB.2017.2714462>.
- [5] Urbanczyk, M., Layland, S.L., Schenke-Layland, K., (2020). The role of extracellular matrix in biomechanics and its impact on bioengineering of cells and 3D tissues. *Matrix Biol.*, **85–86**, 1–14. <https://doi.org/10.1016/j.matbio.2019.11.005>.
- [6] Larin, K.V., Sampson, D.D., (2017). Optical coherence elastography – OCT at work in tissue biomechanics [Invited]. *Biomed. Opt. Express*, **8** (2), 1172. <https://doi.org/10.1364/boe.8.001172>.
- [7] Prevedel, R., Diz-Muñoz, A., Ruocco, G., Antonacci, G., (2019). Brillouin microscopy: an emerging tool for mechanobiology. *Nat. Methods*, **16** (10), 969–977. <https://doi.org/10.1038/s41592-019-0543-3>.
- [8] Gupta, H.S., Seto, J., Krauss, S., Boesecke, P., Screen, H. R.C., (2010). In situ multi-level analysis of viscoelastic deformation mechanisms in tendon collagen. *J. Struct. Biol.*, **169** (2), 183–191. <https://doi.org/10.1016/j.jsb.2009.10.002>.
- [9] Bergholt, M.S., Serio, A., Albro, M.B., (2019). Raman Spectroscopy: Guiding Light for the Extracellular Matrix. *Front. Bioeng. Biotechnol.*, **7** (November), 1–16. <https://doi.org/10.3389/fbioe.2019.00303>.
- [10] Raman, C.V., Krishnan, K.S., (1928). A new type of secondary radiation [11]. *Nature*, **121** (3048), 501–502. <https://doi.org/10.1038/121501c0>.
- [11] Movasaghi, Z., Rehman, S., Rehman, I.U., (2007). Raman spectroscopy of biological tissues. *Appl. Spectrosc. Rev.*, **42** (5), 493–541. <https://doi.org/10.1080/05704920701551530>.
- [12] Bergholt, M.S., Albro, M.B., Stevens, M.M., (2017). Biomaterials Online quantitative monitoring of live cell engineered cartilage growth using diffuse field Raman spectroscopy. *Biomaterials*, **140**, 128–137. <https://doi.org/10.1016/j.biomaterials.2017.06.015>.
- [13] Czamara, K., Majzner, K., Pacia, M.Z., Kochan, K., Kaczor, A., Baranska, M., (2015). Raman spectroscopy of lipids: A review. *J. Raman Spectrosc.*, **46** (1), 4–20. <https://doi.org/10.1002/jrs.4607>.
- [14] Liao, Z. et al, (2017). Feasibility of Spatially Offset Raman Spectroscopy for in Vitro and in Vivo Monitoring Mineralization of Bone Tissue Engineering Scaffolds. *Anal. Chem.*, **89** (1), 847–853. <https://doi.org/10.1021/acs.analchem.6b03785>.
- [15] Kuhar, N., Sil, S., Verma, T., Umapathy, S., (2018). Challenges in application of Raman spectroscopy to biology and materials. *RSC Adv.*, **8** (46), 25888–25908. <https://doi.org/10.1039/c8ra04491k>.
- [16] Green, E., Ellis, R., Winlove, P., (2008). The molecular structure and physical properties of elastin fibers as revealed by Raman microspectroscopy. *Biopolymers*, **89** (11), 931–940. <https://doi.org/10.1002/bip.21037>.
- [17] Martinez, M.G., Bullock, A.J., MacNeil, S., Rehman, I.U., (2019). Characterisation of structural changes in collagen with Raman spectroscopy. *Appl. Spectrosc. Rev.*, **54** (6), 509–542. <https://doi.org/10.1080/05704928.2018.1506799>.
- [18] Puppels, G.J. et al, (Sep. 1990). Studying single living cells and chromosomes by confocal Raman microspectroscopy. *Nature*, **347** (6290), 301–303. <https://doi.org/10.1038/347301a0>.
- [19] Kong, K., Kendall, C., Stone, N., Notinger, I., (2015). Raman spectroscopy for medical diagnostics – From in-vitro biofluid assays to in-vivo cancer detection. *Adv. Drug Deliv. Rev.*, **89**, 121–134. <https://doi.org/10.1016/j.addr.2015.03.009>.
- [20] R. R. Jones, D. C. Hooper, L. Zhang, D. Wolverson, and V. K. Valev, “Raman Techniques: Fundamentals and Frontiers,” *Nanoscale Res. Lett.*, vol. 14, no. 1, 2019, doi: 10.1186/s11671-019-3039-2.
- [21] Camp, C.H., Cicerone, M.T., (2015). Chemically sensitive bioimaging with coherent Raman scattering. *Nat. Photonics*, **9** (5), 295–305. <https://doi.org/10.1038/nphoton.2015.60>.
- [22] J. X. Cheng and X. S. Xie, “Vibrational spectroscopic imaging of living systems: An emerging platform for biology and medicine,” *Science (80-.)*, vol. 350, no. 6264, 2015, doi: 10.1126/science.aaa8870.
- [23] Evans, C.L., Potma, E.O., Puoris’haag, M., Côté, D., Lin, C.P., Xie, X.S., (2005). Chemical imaging of tissue in vivo with video-rate coherent anti-Stokes Raman scattering microscopy. *Proc. Natl. Acad. Sci. U. S. A.*, **102** (46), 16807–16812. <https://doi.org/10.1073/pnas.0508282102>.
- [24] Li, S., Li, Y., Yi, R., Liu, L., Qu, J., (2020). Coherent Anti-Stokes Raman Scattering Microscopy and Its Applications. *Front. Phys.*, **8** (December), 1–9. <https://doi.org/10.3389/fphy.2020.598420>.
- [25] Prince, R.C., Frontiera, R.R., Potma, E.O., (2017). Stimulated Raman scattering: From bulk to nano. *Chem. Rev.*, **117** (7), 5070–5094. <https://doi.org/10.1021/acs.chemrev.6b00545>.
- [26] K. Hashimoto, M. Takahashi, T. Ideguchi, and K. Goda, “Broadband coherent Raman spectroscopy running at 24,000 spectra per second,” *Sci. Rep.*, vol. 6, no. October 2015, pp. 1–7, 2016, doi: 10.1038/srep21036.
- [27] Ozeki, Y. et al, (2012). High-speed molecular spectral imaging of tissue with stimulated Raman scattering. *Nat. Photonics*, **6** (12), 845–851. <https://doi.org/10.1038/nphoton.2012.263>.
- [28] Zipfel, W.R., Williams, R.M., Webb, W.W., (2003). Nonlinear magic: Multiphoton microscopy in the biosciences. *Nat. Biotechnol.*, **21** (11), 1369–1377. <https://doi.org/10.1038/nbt899>.

- [29] Roth, S., Freund, I., (1979). Second harmonic generation in collagen. *J. Chem. Phys.*, **70** (4), 1637–1643. <https://doi.org/10.1063/1.437677>.
- [30] D. Winfried, H. S. James, and Watt W. Webb, “Two-photon laser scanning fluorescence microscopy,” *Science* (80-.), vol. 248, no. April 6, pp. 73–76, 1990, [Online]. Available: <http://www.pubmedcentral.nih.gov/articlerender.fcgi?artid=3481855&tool=pmcentrez&rendertype=abstract>.
- [31] Stelzer, E.H.K. et al, (1994). Nonlinear absorption extends confocal fluorescence microscopy into the ultra-violet regime and confines the illumination volume. *Opt. Commun.*, **104** (4–6), 223–228. [https://doi.org/10.1016/0030-4018\(94\)90546-0](https://doi.org/10.1016/0030-4018(94)90546-0).
- [32] Denk, W., Svoboda, K., (1997). Photon upmanship: Why multiphoton imaging is more than a gimmick. *Neuron*, **18** (3), 351–357. [https://doi.org/10.1016/S0896-6273\(00\)81237-4](https://doi.org/10.1016/S0896-6273(00)81237-4).
- [33] Hopt, A., Neher, E., (2001). Highly nonlinear photodamage in two-photon fluorescence microscopy. *Biophys. J.*, **80** (4), 2029–2036. [https://doi.org/10.1016/S0006-3495\(01\)76173-5](https://doi.org/10.1016/S0006-3495(01)76173-5).
- [34] Wang, T. et al, (2018). Three-photon imaging of mouse brain structure and function through the intact skull. *Nat. Methods*, **15** (10), 789–792. <https://doi.org/10.1038/s41592-018-0115-y>.
- [35] Abdeladim, L. et al, (2019). Multicolor multiscale brain imaging with chromatic multiphoton serial microscopy. *Nat. Commun.*, **10** (1), 1–14. <https://doi.org/10.1038/s41467-019-09552-9>.
- [36] Chen, X., Nadiarynh, O., Plotnikov, S., Campagnola, P. J., (2012). Second harmonic generation microscopy for quantitative analysis of collagen fibrillar structure. *Nat. Protoc.*, **7** (4), 654–669. <https://doi.org/10.1038/nprot.2012.009>.
- [37] Drifka, C.R. et al, (2016). Comparison of Picosirius Red Staining With Second Harmonic Generation Imaging for the Quantification of Clinically Relevant Collagen Fiber Features in Histopathology Samples. *J. Histochem. Cytochem.*, **64** (9), 519–529. <https://doi.org/10.1369/0022155416659249>.
- [38] Van Steenberg, V. et al, (2019). Molecular understanding of label-free second harmonic imaging of microtubules. *Nat. Commun.*, **10** (1), 1–14. <https://doi.org/10.1038/s41467-019-11463-8>.
- [39] Nucciotti, V. et al, (2010). Probing myosin structural conformation in vivo by second-harmonic generation microscopy. *Proc. Natl. Acad. Sci. U. S. A.*, **107** (17), 7763–7768. <https://doi.org/10.1073/pnas.0914782107>.
- [40] Zhuo, Z.Y. et al, (2010). Second harmonic generation imaging – A new method for unraveling molecular information of starch. *J. Struct. Biol.*, **171** (1), 88–94. <https://doi.org/10.1016/j.jsb.2010.02.020>.
- [41] Denk, W., Strickler, J.H., Webb, W.W., (1990). Two-photon laser scanning fluorescence microscopy. *Science* (80-.), **248**(4951), 73–76. <https://doi.org/10.1126/science.2321027>.
- [42] Mansfield, J. et al, (2009). The elastin network: Its relationship with collagen and cells in articular cartilage as visualized by multiphoton microscopy. *J. Anat.*, **215** (6), 682–691. <https://doi.org/10.1111/j.1469-7580.2009.01149.x>.
- [43] Marturano, J.E., Xylas, J.F., Sridharan, G.V., Georgakoudi, I., Kuo, C.K., (2014). Lysyl oxidase-mediated collagen crosslinks may be assessed as markers of functional properties of tendon tissue formation. *Acta Biomater.*, **10** (3), 1370–1379. <https://doi.org/10.1016/j.actbio.2013.11.024>.
- [44] Brasselet, S., (2011). Polarization-resolved nonlinear microscopy: application to structural molecular and biological imaging. *Adv. Opt. Photonics*, **3** (3), 205. <https://doi.org/10.1364/aop.3.000205>.
- [45] Stoller, P., Reiser, K.M., Celliers, P.M., Rubenchik, A.M., (2002). Polarization-modulated second harmonic generation in collagen. *Biophys. J.*, **82** (6), 3330–3342. [https://doi.org/10.1016/S0006-3495\(02\)75673-7](https://doi.org/10.1016/S0006-3495(02)75673-7).
- [46] Hung, C.W. et al, (2021). Label-Free Characterization of Collagen Crosslinking in Bone-Engineered Materials Using Nonlinear Optical Microscopy. *Microsc. Microanal.*, 1–11. <https://doi.org/10.1017/S1431927621000295>.
- [47] Pittet, J.C., Freis, O., Vazquez-Duchêne, M.D., Périé, G., Pauly, G., (2014). Evaluation of elastin/collagen content in human dermis in-vivo by multiphoton tomography-variation with depth and correlation with aging. *Cosmetics*, **1** (3), 211–221. <https://doi.org/10.3390/cosmetics1030211>.
- [48] Raub, C.B., Mahon, S., Narula, N., Tromberg, B.J., Brenner, M., George, S.C., (2010). Linking optics and mechanics in an in vivo model of airway fibrosis and epithelial injury. *J. Biomed. Opt.*, **15**, (1) <https://doi.org/10.1117/1.3322296> 015004.
- [49] Raub, C.B., Putnam, A.J., Tromberg, B.J., George, S.C., (2010). Predicting bulk mechanical properties of cellularized collagen gels using multiphoton microscopy. *Acta Biomater.*, **6** (12), 4657–4665. <https://doi.org/10.1016/j.actbio.2010.07.004>.
- [50] Mercatelli, R. et al, (2019). Morpho-mechanics of human collagen superstructures revealed by all-optical correlative micro-spectroscopies. *Commun. Biol.*, **2** (1), 1–10. <https://doi.org/10.1038/s42003-019-0357-y>.
- [51] Lynch, B. et al, (2017). A novel microstructural interpretation for the biomechanics of mouse skin derived from multiscale characterization. *Acta Biomater.*, **50**, 302–311. <https://doi.org/10.1016/j.actbio.2016.12.051>.
- [52] Chow, M.J., Turcotte, R., Lin, C.P., Zhang, Y., (2014). Arterial extracellular matrix: A mechanobiological study of the contributions and interactions of elastin and collagen. *Biophys. J.*, **106** (12), 2684–2692. <https://doi.org/10.1016/j.bpj.2014.05.014>.
- [53] Mansfield, J.C., Bell, J.S., Winlove, C.P., (2015). The micromechanics of the superficial zone of articular cartilage. *Osteoarthr. Cartil.*, **23** (10), 1806–1816. <https://doi.org/10.1016/j.joca.2015.05.030>.
- [54] Gusachenko, I., Tran, V., Houssen, Y.G., Allain, J.M., Schanne-Klein, M.C., (2012). Polarization-resolved second-harmonic generation in tendon upon mechanical stretching. *Biophys. J.*, **102** (9), 2220–2229. <https://doi.org/10.1016/j.bpj.2012.03.068>.
- [55] C. Cavinato, S. Il Murtada, A. Rojas, and J. D. Humphrey, “Evolving structure-function relations during aortic maturation and aging revealed by multiphoton microscopy,” *Mech. Ageing Dev.*, vol. 196, no. March, p. 111471, 2021, doi: 10.1016/j.mad.2021.111471.
- [56] Bergholt, M.S. et al, (2016). Raman spectroscopy reveals new insights into the zonal organization of native and tissue-engineered articular cartilage. *ACS Cent. Sci.*, **2** (12), 885–895. <https://doi.org/10.1021/acscentsci.6b00222>.

- [57] Mansfield, J., Moger, J., Green, E., Moger, C., Winlove, C. P., (2013). Chemically specific imaging and in-situ chemical analysis of articular cartilage with stimulated Raman scattering. *J. Biophotonics*, **814** (10), 803–814. <https://doi.org/10.1002/jbio.201200213>.
- [58] Krafft, C. et al, (2021). Monitoring changes in biochemical and biomechanical properties of collagenous tissues using label-free and nondestructive optical imaging techniques. *Anal. Chem.*, **93** (8), 3813–3821. <https://doi.org/10.1021/acs.analchem.0c04306>.
- [59] Mattson, J.M., Turcotte, R., Zhang, Y., (2017). Glycosaminoglycans contribute to extracellular matrix fiber recruitment and arterial wall mechanics. *Biomech. Model. Mechanobiol.*, **16** (1), 213–225. <https://doi.org/10.1007/s10237-016-0811-4>.
- [60] Labroo, P. et al, (2021). Physical characterization of swine and human skin: Correlations between Raman spectroscopy, Tensile testing, Atomic force microscopy (AFM), Scanning electron microscopy (SEM), and Multiphoton microscopy (MPM). *Ski. Res. Technol.*, **27** (4), 501–510. <https://doi.org/10.1111/srt.12976>.
- [61] Pezzotti, G., (2005). Raman piezo-spectroscopic analysis of natural and synthetic biomaterials. *Anal. Bioanal. Chem.*, **381**, 577–590. <https://doi.org/10.1007/s00216-004-2780-1>.
- [62] Brauchle, E. et al, (2018). Biomechanical and biomolecular characterization of extracellular matrix structures in human colon carcinomas. *Matrix Biol.*, **68–69** (2018), 180–193. <https://doi.org/10.1016/j.matbio.2018.03.016>.
- [63] Raub, C.B. et al, (2007). Noninvasive assessment of collagen gel microstructure and mechanics using multiphoton microscopy. *Biophys. J.*, **92** (6), 2212–2222. <https://doi.org/10.1529/biophysj.106.097998>.
- [64] Robertson, C., Ikemura, K., Krasieva, T.B., George, S.C., (2013). Multiscale analysis of collagen microstructure with generalized image correlation spectroscopy and the detection of tissue prestress. *Biomaterials*, **34** (26), 6127–6132. <https://doi.org/10.1016/j.biomaterials.2013.04.019>.
- [65] Quigley, A.S., Bancelin, S., Deska-Gauthier, D., Légaré, F., Kreplak, L., Veres, S.P., (2018). In tendons, differing physiological requirements lead to functionally distinct nanostructures. *Sci. Rep.*, **8** (1), 1–14. <https://doi.org/10.1038/s41598-018-22741-8>.
- [66] Abraham, T., Fong, G., Scott, A., (2011). Second harmonic generation analysis of early Achilles tendinosis in response to in vivo mechanical loading. *BMC Musculoskelet. Disord.*, **12** <https://doi.org/10.1186/1471-2474-12-26>.
- [67] Bah, I., Fernandes, N.R.J., Chimenti, R.L., Ketz, J., Flemister, A.S., Buckley, M.R., (2020). Tensile mechanical changes in the Achilles tendon due to Insertional Achilles tendinopathy. *J. Mech. Behav. Biomed. Mater.*, vol. **112**, no. **August**, <https://doi.org/10.1016/j.jmbbm.2020.104031> 104031.
- [68] B. R. Freedman et al., “Tendon healing affects the multiscale mechanical, structural and compositional response of tendon to quasi-static tensile loading,” *J. R. Soc. Interface*, vol. 15, no. 139, 2018, doi: 10.1098/rsif.2017.0880.
- [69] E. Hase, T. Minamikawa, K. Sato, D. Yonekura, M. Takahashi, and T. Yasui, “Quantitative Evaluation of Both Histological and Mechanical Recovery in Injured Tendons Using Fourier-Transform Second-Harmonic Generation Microscopy,” *IEEE J. Sel. Top. Quantum Electron.*, vol. 27, no. 4, 2021, doi: 10.1109/JSTQE.2021.3063535.
- [70] Gasior-Głogowska, M. et al, (2013). FT-Raman spectroscopic study of human skin subjected to uniaxial stress. *J. Mech. Behav. Biomed. Mater.*, **18**, 240–252. <https://doi.org/10.1016/j.jmbbm.2012.11.023>.
- [71] Woessner, A.E., Jones, J.D., Witt, N.J., Sander, E.A., Quinn, K.P., (2021). Three-Dimensional Quantification of Collagen Microstructure During Tensile Mechanical Loading of Skin. *Front. Bioeng. Biotechnol.*, **9** (March), 1–11. <https://doi.org/10.3389/fbioe.2021.642866>.
- [72] Bell, J.S. et al, (2016). Microstructure and mechanics of human resistance arteries. *Am. J. Physiol. – Hear. Circ. Physiol.*, **311** (6), H1560–H1568. <https://doi.org/10.1152/ajpheart.00002.2016>.
- [73] Sugita, S., Matsumoto, T., (2017). Multiphoton microscopy observations of 3D elastin and collagen fiber microstructure changes during pressurization in aortic media. *Biomech. Model. Mechanobiol.*, **16** (3), 763–773. <https://doi.org/10.1007/s10237-016-0851-9>.
- [74] Chen, H. et al, (2013). Biaxial deformation of collagen and elastin fibers in coronary adventitia. *J. Appl. Physiol.*, **115** (11), 1683–1693. <https://doi.org/10.1152/jappphysiol.00601.2013>.
- [75] W. Krasny, H. Magoaric, C. Morin, and S. Avril, “Kinematics of collagen fibers in carotid arteries under tension-inflation loading,” *J. Mech. Behav. Biomed. Mater.*, vol. 77, no. May 2017, pp. 718–726, 2018, doi: 10.1016/j.jmbbm.2017.08.014.
- [76] Bell, J.S., Christmas, J., Mansfield, J.C., Everson, R.M., Winlove, C.P., (Jun. 2014). Micromechanical response of articular cartilage to tensile load measured using nonlinear microscopy. *Acta Biomater.*, **10** (6), 2574–2581. <https://doi.org/10.1016/j.actbio.2014.02.008>.
- [77] J. C. Mansfield, V. Mandalia, A. Toms, C. Peter Winlove, and S. Brasselet, “Collagen reorganization in cartilage under strain probed by polarization sensitive second harmonic generation microscopy,” *J. R. Soc. Interface*, vol. 16, no. 150, 2019, doi: 10.1098/rsif.2018.0611.
- [78] Beaulieu, D.R., Davison, I.G., Kılıç, K., Bifano, T.G., Mertz, J., (2020). Simultaneous multiplane imaging with reverberation two-photon microscopy. *Nat. Methods*, **17** (3), 283–286. <https://doi.org/10.1038/s41592-019-0728-9>.
- [79] S. Leemans, A. Dvornikov, T. Gallagher, and E. Gratton, “AO DIVER: Development of a three-dimensional adaptive optics system to advance the depth limits of multiphoton imaging,” *APL Photonics*, vol. 5, no. 12, 2020, doi: 10.1063/5.0032621.
- [80] Gong, L., Zheng, W., Ma, Y., Huang, Z., (2020). Higher-order coherent anti-Stokes Raman scattering microscopy realizes label-free super-resolution vibrational imaging. *Nat. Photonics*, **14** (2), 115–122. <https://doi.org/10.1038/s41566-019-0535-y>.
- [81] Lilledahl, M.B., Pierce, D.M., Ricken, T., Holzapfel, G.A., Davies, C.D.L., (2011). Structural analysis of articular cartilage using multiphoton microscopy: Input for biomechanical modeling. *IEEE Trans. Med. Imaging*, **30** (9), 1635–1648. <https://doi.org/10.1109/TMI.2011.2139222>.
- [82] Jayyosi, C., Fargier, G., Coret, M., Bruyère-Garnier, K., (2014). Photobleaching as a tool to measure the local strain field in fibrous membranes of connective tissues.

- Acta Biomater.*, **10** (6), 2591–2601. <https://doi.org/10.1016/j.actbio.2014.02.031>.
- [83] Thunes, J.R. et al, (2016). A structural finite element model for lamellar unit of aortic media indicates heterogeneous stress field after collagen recruitment. *J. Biomech.*, **49** (9), 1562–1569. <https://doi.org/10.1016/j.jbiomech.2016.03.034>.
- [84] A. Lombardini et al., “High-resolution multimodal flexible coherent Raman endoscope article,” *Light Sci. Appl.*, vol. 7, no. 1, 2018, doi: 10.1038/s41377-018-0003-3.
- [85] Sherlock, B. et al, (2018). In vivo multiphoton microscopy using a handheld scanner with lateral and axial motion compensation. *J. Biophotonics*, **11** (2), 1–10. <https://doi.org/10.1002/jbio.201700131>.
- [86] Liang, W., Hall, G., Messerschmidt, B., Li, M.J., Li, X., (2017). Nonlinear optical endomicroscopy for label-free functional histology in vivo. *Light Sci. Appl.*, **6** (11), e17082–7. <https://doi.org/10.1038/lsa.2017.82>.